Symmetry, Integrability and Geometry: Methods and Applications Vol. 2 (2006), Paper 015, 7 pages

Auger Spectra and Different Ionic Charges Following $3s$, $3p$ and $3d$ Sub-Shells Photoionization of Kr Atoms

Yehia A. LOTFY † *and Adel M. El-SHEMI* ‡

† *Physics Department, Faculty of Science, El Minia University, P.O. Box 61111, El Minia, Egypt*
E-mail: *yahialotfy59@yahoo.com*

‡ *Applied Sciences Department, College of Technological Studies, P.O. Box 42325, Shuwaikh, 70654 Kuwait*
E-mail: *admohamed@yahoo.com*

Received August 21, 2005, in final form January 15, 2006; Published online January 31, 2006
Original article is available at http://www.emis.de/journals/SIGMA/2006/Paper015/

Abstract. The decay of inner-shell vacancy in an atom through radiative and non-radiative transitions leads to final charged ions. The de-excitation decay of $3s$, $3p$ and $3d$ vacancies in Kr atoms are calculated using Monte–Carlo simulation method. The vacancy cascade pathway resulted from the de-excitation decay of deep core hole in $3s$ subshell in Kr atoms is discussed. The generation of spectator vacancies during the vacancy cascade development gives rise to Auger satellite spectra. The last transitions of the de-excitation decay of $3s$, $3p$ and $3d$ holes lead to specific charged ions. Dirac–Fock–Slater wave functions are adapted to calculate radiative and non-radiative transition probabilities. The intensity of Kr^{4+} ions are high for $3s$ hole state, whereas Kr^{3+} and Kr^{2+} ions have highest intensities for $3p$ and $3d$ hole states, respectively. The present results of ion charge state distributions agree well with the experimental data.

Key words: ion charge state distributions; highly charged ions

2000 Mathematics Subject Classification: 81V45

1 Introduction

The relaxation of inner-shell ionized atom via successive Auger, Coster–Kronig and radiative transitions leads to production of highly charged ions. In the course of de-excitation decay pathway, multiple vacancies are generated after each Auger transition. The distribution of generated vacancies does not dependent on the initial ionization process. The Auger cascades are accompanied with emission of photon spectra or electron spectra for each pathway branch. The spectra are conditioned by the transition rates and transition energies of multi-vacancy states. The generation of vacancies in the course of de-excitation cascade is accompanied by characteristic energy shifts in the electronic levels. The influence of the additional vacancies during the cascades may close some low-energy Auger channels (forbidden energies). Understanding the influence of the spectator vacancies on Auger transitions, gives more detailed information about the vacancy cascade development. The overlapping spectra emitted from parallel branches of the de-excitation cascades lead to different low-energy highly charged ions. These low-energy ionic charges are important in the field of astrophysical plasma [1]. Study of ion charge state distributions following inner-shell ionization of atoms provides information to estimate the characteristic relaxation time constants and thermal equilibrium of ion gas that stored in trap [2, 3, 4]. The ion charge state distributions following inner-shell ionized rare gas atoms are measured using both energy ionization from x-ray tube [5, 6], and synchrotron radiation [7, 8, 9, 10, 11]. Tamenori et al. [12] measured the branching ratio of multiply charged ions formed through photoionization of Kr $3d$, $3p$ and $3s$ subshells using a coincidence technique. The calculations of ion charge state distributions resulted after core-hole creation of atom are carried out by many researchers [13, 14, 15, 16, 17, 18, 19, 20, 21, 22].

The Auger transition rates and transition energies in multi-ionized neon atom are measured using heavy-ion and electron bombardment [23] and calculated using Hartree–Fock–Slater wave functions [24]. Larkins [25] investigated the influence of multi-vacancy states on the electron binding energies and transition rates in K, L, and M subshells in the calculation of ion charge state distributions. Auger and x-ray spectra formed during vacancy cascades are calculated using Monte–Carlo method [26, 27]. Cooper et al. [28] measured and calculated the $L_{23}MM$ Auger spectra of argon excited at energies between those of K- and L-thresholds and affected by $L_1L_{23}M$ intermediate transition. The $L_{23}MM$ Auger spectra of argon emitted after photoexcitation are measured using broad-band synchrotron radiation of energies largely lying above the K-shell ionization potential [29].

In the present work, the different ionic charges followed $3s$, $3p$ and $3d$ subshells photoionization of Kr are calculated using Monte Carlo simulation technique. The calculation is considered an extension to the previous work carried out by Abdullah et al. [21], in which ion charge state distributions yield after $1s$, $2s$ and $2p$ vacancy creation in Kr atoms are obtained. The de-excitation decay branches of parallel Coster–Kronig and Auger transitions followed $3s$, $3p$ and $3d$ hole production are discussed. The Auger transition rates and electron shake off are obtained using Dirac–Fock–Slater wave functions. The present results are compared with available theoretical [16] and experimental values [12].

2 Method of calculations

The highly excited atoms resulted after electron emission from inner-shell will rapidly relax back to a lower energy state by radiative or non-radiative process. In case of radiative transition, the vacancy transfers to a higher shell under emission of characteristic x-rays:

$$A + h\nu \longrightarrow (A^{1+})^* + e_p \longrightarrow (A^{1+})^* \longrightarrow A^{1+} + h\nu',$$

where the core hole in the target atom A is produced by photoionization ($h\nu$), $(A^{1+})^\star$ is the atom in highly excited state and e_p is the primary emitted electron. If the vacancy is filled via Auger transition, two vacancies in the higher shells of atom will be created and the transition is given by:

$$A + h\nu \longrightarrow (A^{1+})^* + e_p \longrightarrow (A^{1+})^* \longrightarrow A^{2+} + e_{\text{Auger}},$$

where A^{2+} is doubly ionized atom.

In an Auger transition, one electron falls from a higher level to fill the initial vacancy and another electron is ejected into continuum. The kinetic energy of emitted Auger electron can be estimated from the binding energies of the various levels involved in the transition:

$$E_{Kin} = E_i - (E_j + E_k),$$

where E_i is the binding energy of initial state, E_j is the binding energy of electron filling the hole and E_k is the binding energy of the electron leaving the atom.

The simulation of the cascade branches is based on the selection of all possible radiative and non-radiative branching ratios that may fill the inner-shell vacancies in atoms. The radiative branching ratio is defined as the probability that the vacancy in an atom is filled through x-ray transitions (photon emission), while the non-radiative branching ratio is defined as the vacancy filled through Auger and Coster–Kronig processes. The radiative and non-radiative branching ratio are given by:

For fluorescence yield:

$$\omega(f \longrightarrow i) = \Gamma^R_{if}/\Gamma$$

and for Auger yield:

$$\omega(f \longrightarrow i) = \Gamma^A_{if}/\Gamma,$$

where i is the initial configuration decaying into the final configuration f. Γ is the sum of partial radiative widths Γ^R_{if} and non-radiative width Γ^A_{if} which is given by:

$$\Gamma = \sum_{i,f} \Gamma^R_{if} + \sum_{i,f} \Gamma^A_{if}.$$

The calculations of radiative transition rates are performed for singly ionized atoms using multiconfiguration-Dirac–Fock (MCDF) wave functions [30]. The non-radiative transition rates and electron shake off processes are computed using Dirac–Fock–Slater (DFS) wave functions [31].

The Monte–Carlo simulation technique is described in detail by Abdullah et al. [21], in which the electron shake off process is considered. In radiative transitions case, the inner-shell vacancy will transfer to higher shell under emission of characteristic x-rays without changing the number of vacancies thus a new position of vacancy is created. If the vacancy is filled via Auger process, two vacancies in the higher shells of atom will be generated. The de-excitation decays are repeated until all vacancies reach the outermost shell and no transitions are possible. The successive Auger cascades lead to the production of specified low-energy charged ions. The Auger cascades correspond to transitions with emission of photon spectra or electron spectra for each pathway branches. In the course of cascade development, Auger spectra arise from spectator vacancies left by preceding Auger transitions and by electron shake off process accompanying the Auger transitions.

3 Results and discussions

Fig. 1 shows a schematical diagram for all main de-excitation decay pathway resulted after $3s$ vacancy creation in Kr atom. The solid arrows indicate the selected Auger channels following inner-shell ionization, while dotted ones show the Coster–Kronig channels. The solid line indicates the radiative transition; while dotted lines indicate the electron shake off processes occuring due to the change of atomic potential after primary ionization or after Auger and Coster–Kronig transitions. Electron shake off process resulted from the initial ionization or de-excitation decay produces additional vacancies in higher shells leading to an increase in the number of vacancies. Auger and Coster–Kronig transitions are indicated outside the brackets, while the spectator vacancy configurations are indicated inside the brackets. Each branch of the de-excitation leads to an ion of a specific charge as shown in the diagram. Considering of electron shake off process in the calculation gives a final charge state of ions which agree well with the experimental data.

Fig. 2 shows the charge state of ions resulted after $3s$ vacancy creation in Kr atoms. The present results are compared with other theoretical values from Kochur et al. [16] and experimental data from Tamenori et al. [12]. The relaxation of ionized atom occurs through radiative and/or non-radiative transitions. At $3s$ hole state in Kr atoms, the probability of radiative transitions is lower than the probability of non-radiative transitions. The radiative branching ratios will occur in 1 % of the cases as given by the fluorescence yield. In the remaining 99 % of the

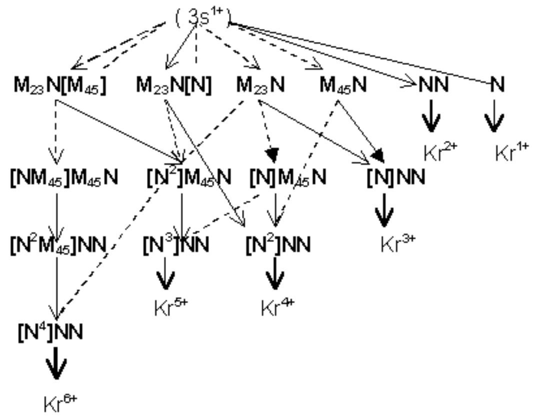

Figure 1. Decay branches pathway after $3s$ vacancy production in Kr atom.

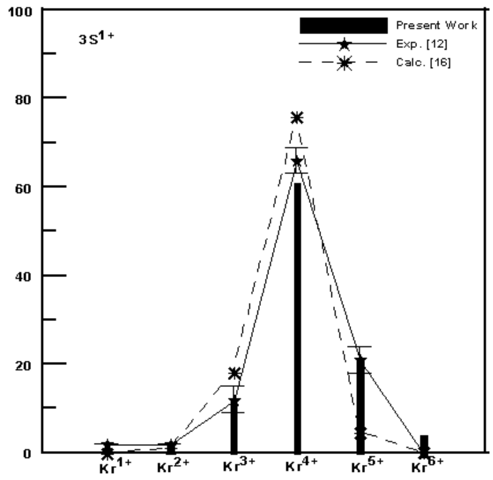

Figure 2. Different ionic charges formed following $3s$ shell ionization in Kr atom.

cases, the $3s$ vacancy is filled by non-radiative processes (Auger and Coster–Kronig transitions). The ionization of the N valence electron through radiative transitions leads to the formation of Kr^{1+} ions. The intensity of singly charged ions followed $3s$ hole creation is less than 1 %. The $3s$ hole is filled by one of three possible $\mathrm{M_1M_{23}N}$, $\mathrm{M_1M_{45}}N$ Coster–Kronig transitions and $\mathrm{M_1NN}$ Auger transition. At $3s$ hole state, the probability of super Coster–Kronig transitions $\mathrm{M_1MM}$ is lower than the probability of Auger and Coster–Kronig transitions. The decay of $3s$ vacancy through Auger or Coster–Kronig channel will create an additional vacancy in N subshells. The generation of N vacancy produced during vacancy cascade leads to characteristic energy shifts in the energy levels. This additional N vacancy closes low-energy super Coster–Kronig $\mathrm{M_1MM}$ channels and these channels become energy forbidden. The relative transition probability (branching ratio) for $\mathrm{M_1M_{23}N}$, $\mathrm{M_1M_{45}N}$ and $\mathrm{M_1NN}$ decays are 72 %, 26 % and 1.5 %, respectively. The intensity of doubly charged ions Kr^{2+} at $3s$ hole state is about 2 %. The yield of Kr^{3+} ions with intensity of 12 % arises from Coster–Kronig channels and subsequent Auger transitions following $3s$ hole creation. The formation of Kr^{4+} is caused by initial $\mathrm{M_1M_{23}N}$ Coster–Kronig transition and subsequent Coster–Kronig transition from $\mathrm{M_{23}M_{45}N}$ shell and $\mathrm{M_{45}NN}$ Auger transition. During the vacancy cascade de-excitation, the intensity of $\mathrm{M_{45}NN}$ Auger spectra with additional $[\mathrm{N}^2]$ vacancies is high. The $3s$ ionization significantly produces quadruply charged (Kr^{4+}) ions via Coster–Kronig decays with subsequent Auger transitions. The intensity of quadruply charged ions resulted from 3s vacancy is 61 %. The spectator vacancies [N] decrease the energy of $\mathrm{M_{45}NN}$ Auger transition by several electron volts. This is because the spectator vacancies change the shielding of the M and N levels. The strongest line spectrum arise from $\mathrm{M_{45}[N^2] - NN[N^2]}$ transitions and leads to a stable Kr^{4+} ions. The Kr^{5+} and Kr^{6+} ions are formed from the de-excitation via parallel Auger and Coster–Kronig channels and electron shake off process. The intensities of the Kr^{5+} and Kr^{6+} ions are 21 % and less than 4 %, respectively. It is found that the creation of additional N vacancies during the de-excitation decay of $3s$ hole closes the $\mathrm{M_{23}M_{45}M_{45}}$ super Coster–Kronig channel, i.e. the super Coster–Kronig transition energy is forbidden. The intensity of Kr^{4+} and Kr^{5+} ions is high while a Kr^{1+}, Kr^{2+}, Kr^{3+} and Kr^{6+} ions is low. The most probable de-excitation pathway of a $3s$ shell vacancy is via Coster–Kronig transitions, which will create $\mathrm{M_{45}}$ vacancies with additional N sub-shell vacancies. So each spectator vacancy configuration will give rise to an $\mathrm{M_{45}NN}$ satellite spectrum. The present results of ion charge state distributions after $3s$ vacancy production agree well with the experimental data [12].

The ion charge state distributions produced after $3p$ hole creation in Kr are shown in Fig. 3. The de-excitation decay of $3p$ hole gives rise to different ionic charges Kr^q, $q = 1, \ldots, 5$. The

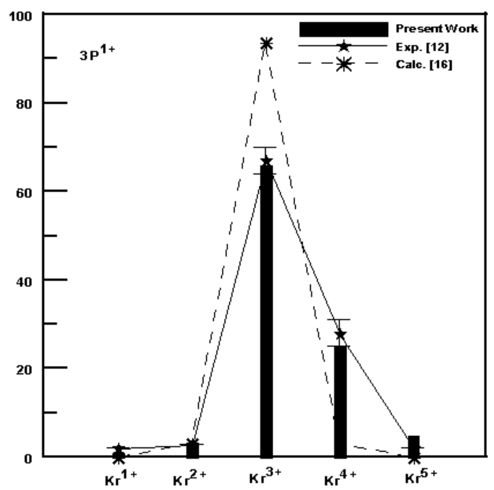

Figure 3. Different ionic charged following $3p$ shell ionization in Kr atom.

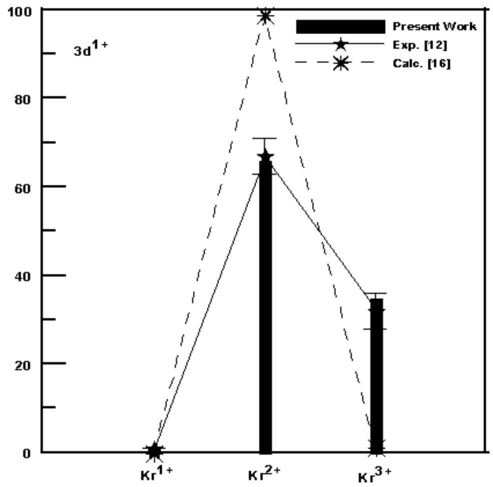

Figure 4. Different ionic charged following $3d$ shell ionization in Kr atom.

$3p$ hole is filled by one of the following possible transitions: $M_{23}M_{45}M_{45}$ super Coster–Kronig, $M_{23}M_{45}N$ Coster–Kronig and $M_{23}NN$ Auger transitions. The relative transition probability (branching ratio) for $M_{23}M_{45}M_{45}$, $M_{23}M_{45}N$ and $M_{23}NN$ decays are 61 %, 29 % and 2 %, respectively. In the $3p$ hole state, the ionization of the $3p$ electrons increases the intensity of triply charged ions Kr^{3+} and decreases the quadruply charged ions Kr^{4+} in comparison with the corresponding charged ions that produced after $3s$ vacancy. The formation of Kr^{1+} is caused by radiative transition with ionizing electron from N subshells. The intensity of Kr^{1+} ions after $3p$ shell ionization is less than 1 %. The decay of $3p$ vacancy via normal $M_{23}NN$ Auger transition leads to the formation of doubly charged ions Kr^{2+} with an intensity of 3 %. The formation of Kr^{3+} ions occurs from the decay of $3p$ hole via initial Coster–Kronig channel and subsequent Auger transition. The triply charged ions Kr^{3+} followed after the $3p$ ionization has highest intensity (66 %). The Kr^{4+} ions with intensity of 25 % are formed via Coster–Kronig, Auger transitions and electron shake-off from N shell. The probability of electron shake off from N shell after $3p$ ionization is about 7 %. The intensity of Kr^{5+} ions yields from vacancy cascade followed $3p$ hole production is 5 %. In general, the de-excitation decay of $3p$ hole of Kr leads to dominant production of Kr^{3+} and Kr^{4+} charged ions and lower production of Kr^{2+} and Kr^{5+} ions, respectively.

The percentage fraction of the ion charge state distributions yields from de-excitation decay of $3d$ hole in Kr are shown in Fig. 4. The highest intensity Kr^{2+} ions formed from de-excitation decays of $3d$ photoionization. The de-excitation decays of $3d$ vacancy yields Kr^{2+} with higher intensity and Kr^{3+} ions with lower intensity in comparison with the corresponding results from $3p$ vacancy. The intensities of doubly and triply charged ions are 66 % and 35 %, respectively. It is important to mention that the present results of ion charge state distributions produced after $3s$, $3p$ and $3d$ vacancies production in Kr atoms agree well with the experimental data from Tamenori et al. [12].

4 Conclusions

The core hole creation followed by successive Auger, Coaster–Kronig transitions and electron shake off leads to different ionic charge. Monte Carlo simulation method is performed to calculate the highly charged ions after $3s$, $3p$ and $3d$ vacancies creation in Kr atom. The Auger and Coster–Kronig branching ratio and electron shake off process are calculated using Dirac–Fock–Slater wavefunctions. The cascade of decay pathway branches followed $3s$, $3p$ and $3d$ holes are discussed. The Kr^{4+} ions have highest intensity in the $3s$ shell ionization, while Kr^{3+} and Kr^{2+} ions have the highest intensity in the $3p$ and $3d$ shell ionization, respectively. The present results are compared with other theoretical values [16] and experimental [12] and are found to agree well with the experimental values.

[1] McDowell M.R.C., Ferendici A.M., Atomic and molecular processes in controlled thermonulear fusion, New York, Plenum, 1980.

[2] Church D.A., Kravis S.D., Sellin I.A., Levin J.C., Short R.T., Meron M., Johnson B.M., Jones K.W., Confined thermal multicharged ions produced by synchrotron radiation, *Phys. Rev. A*, 1987, V.36, 2487–2490.

[3] Church D.A., Kravis S.D., Sellin I.A., Levin J.C., Short R.T., Meron M., Johnson B.M., Jones K.W., Confined thermal multicharged ions produced by synchrotron radiation, *Phys. Rev. A*, 1987, V.36. 2487–2490.

[4] Kravis S.D., Church D.A., Johnson B.M., Sellin I.A., Azuma Y., Mansour N., Berry H.G., Inner-shell photoionization of stored positive ions using synchrotron radiation, *Phys. Rev. Lett.*, 1991, V.66, 2956–2959.

[5] Carlson T.A., Krause M.O., Atomic readjustment to vacancies in the K and L shells of argon, *Phys. Rev. A*, 1965, V.137, 1655–1662.

[6] Krause M.O., Carlson T.A., Vacancy cascade in the reorganization of Krypton ionized in an inner shell, *Phys. Rev.*, 1967, V.158, 18–24.

[7] Ueda K., Shigemasa E., Sato T., Yagishita A., Ukai M., Maezawa H., Hayaishi T., Sasaki T., Threshold behaviour of the multiply charged photoion yields near the Ar K edge, *J. Phys. B: At. Mol. Opt. Phys.*, 1991, V.24, 605–613.

[8] Hayaishi T., Morioka Y., Kageyama Y., Watanabe M., Suzuki I.H., Mikuni A., Isoyama G., Asaoka S., Nakamura M., Multiple photoionisation of the rare gases in the XUV region, *J. Phys. B: At. Mol. Phys.*, 1987, V.20, 3511–3527.

[9] Mukoyama T., Tonuma T., Yagishita A., Shibata H., Matsuo T., Shima K., Tawara H., Charge distribution of Xe ions as a result of multiple photoionisation of Xe atoms between 4.1 and 8.0 keV, *J. Phys. B: At. Mol. Phys.*, 1987, V.20, 4453–4460.

[10] Saito N., Suzuki I.H., Yields of multicharged Xe ions in the M-shell transition region, *J. Phys. B: At. Mol. Opt. Phys.*, 1992, V.25, 1785–1793.

[11] Tawara H., Hayaishi T., Koizumi T., Matsuo T., Shima K., Yagishita A., Production of multiply charged Xei+ ions via photoionization and excitation in the L-edge region, *J. Phys. B: At. Mol. Opt. Phys.*, 1992, V.25, 1467–1473.

[12] Tamenori Y., Okada K., Tanimoto S., Ibuki T., Nagaoka S., Fujii A., Haga Y., Suzuki I.H., Branching ratios of multiply charged ions formed through photoionization of Kr $3d$, $3p$ and $3s$ sub-shells using a coincidence technique, *J. Phys. B: At. Mol. Opt. Phys.*, 2004, V.37, 117–129.

[13] Omar G., Hahn Y., Cascade decay of hollow ions, *Phys. Rev. A*, 1991, V.43, 4695–4701.

[14] Omar G., Hahn Y., Photo-auger – ionization and charge-state distribution, *Phys. Rev. A*, 1991, V.44, 483–488.

[15] Kochur A.G., Dudenko A.I., Sukhorukov V.L., Petrov I.D., Direct Hartree–Fock calculation of multiple Xei+ ion production through inner-shell vacancy de-excitations, *J. Phys. B: At. Mol. Opt. Phys.*, 1994, V.27, 1709–1721.

[16] Kochur A.G., Dudenko A.I., Sukhorukov V.L, Petrov I.D., Direct Hartree–Fock calculation of the cascade decay production of multiply charged ions following inner-shell ionization of Ne, Ar, Kr, and Xe, *J. Phys. B: At. Mol. Opt. Phys.*, 1995, V.28, 387–402.

[17] Opendak M.G., Auger cascades in atoms and ions of astrophysically important elements, *Astrophys. and Space Sci.*, 1990, V.165, 9–25.

[18] Mukoyama T., Vacnacy cascade following inner-shell ionization, *Bull. Inst. Chem. Res. Kyoto Univ.*, 1985, V.63, 373–382.

[19] Mirakhmedove M.N., Parilis E.S., Auger and x-ray cascades following inner-shell ionization, *J. Phys. B: At. Mol. Opt. Phys.*, 1988, V.21, 795–804.

[20] El-Shemi A.M., Ghoneim A.A., Lotfy Y.A., Multiply charged ions produced after deexcitation processes for important elements in astrophysics, *Turk. J. Phys.*, 2003, V.27, 51–59.

[21] Abdullah A.H., El-Shemi A.M., Ghoneim A.A., Yields of multiply charged ions produced from inner-shell ionization in neutral Ne, Ar, and Kr atoms, *Radia. Phys. Chem.*, 2003, V.68, 697–705.

[22] El-Shemi A.M., Lotfy Y.A., Ion charge state distributions following K-shell ionization in atoms, *Eur. Phys. J. D*, 2005, V.31, 1–7.

[23] Matthews D.L., Johnson B.M., Mackey J.J., Moore C.F., High-resolution K-Auger spectra for multiply ionized neon, *Phys. Rev. Lett.*, 1973, V.31, 331–334.

[24] Bhalla C.P., Folland N.O., Hein M.A., Theoretical K-shell Auger rates, transition energies and fluorescence yields for multiply ionized neon, *Phys. Rev. A.*, 1973, V.8, 649–657.

[25] Larkins F.P., Dependence of fluorescence yields on atomic configuration, *J. Phys. B: At. Mol. Phys.*, 1971, V.4, L29–L32.

[26] Mirakhmedov M.N., Auger and x-ray spectra formed at highly charged ion neutralization near the metal surface, *Nucl. Inst. Methods Phys. Research B*, 1995, V.98, 429–435.

[27] Mirakhmedove M.N., Parilis E.S., Energy of atoms with several vacancies in inner shells, *J. Phys. B: At. Mol. Opt. Phys.*, 1988, V.21, 775–793.

[28] Cooper J.W., Southworth S.H., MacDonald M.A., LeBrun T., Cascade effects on the Ar LMM Auger spectrum, *Phys. Rev. A*, 1994, V.50, 405–412.

[29] Von Busch F., Doppelfeld J., Gunther C., Hartmann E., Argon L23-MM Auger satellite spectrum emitted after K ionization, *J. Phys. B: At. Mol. Opt. Phys.*, 1994, V.27, 2151–2160.

[30] Grant I.P., Mckenzie B.J., Norrington P., Mayers D.F., Pyper N.C., An atomic multiconfigurational Dirac–Fock package, *Comput. Commun.*, 1980, V.21, 207–231.

[31] Lorenz M., Hartmann E., Effect of L-shell spectator vacancy on x-ray fluorescence yield and relative intensities, *J. Phys. B: At. Mol. Phys.*, 1987, V.20, 6189–6195.